tracted from (3) we have

$$(\theta_{41} - \theta_{14}) + (\theta_{23} - \theta_{32}) + (\theta_{12} - \theta_{21}) + (\theta_{34} - \theta_{43}) = 0. \quad (4)$$

In the reciprocal case the bracketed terms of (4) are separately zero.

It is interesting to observe the specific manner in which the nonreciprocal character of the device is permitted, by the constraints, to display itself. We note from (1) that the magnitude of the forward coupling between one port (say port 1) and a second port (say port 4) must equal the magnitude of the forward coupling between the port isolated from the first port (port 3) and the port isolated from the second port (port 2). See Fig. 1. A similar statement holds for the backward coupling. Thus, some degree of symmetry is preserved; lack of reciprocity manifesting itself only in the fact that the forward and backward coupling need not be equal, and $\theta_{ij} \neq \theta_{ji}$.

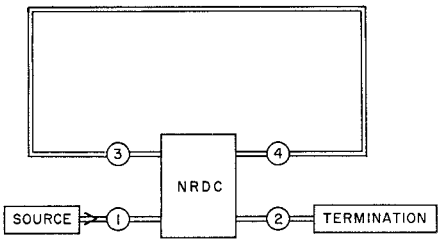

Fig. 1. Traveling-wave resonator utilizing a nonreciprocal directional coupler.

A NRDC may also be considered a generalization of a circulator, and can be usefully viewed as a means of describing an imperfect circulator.

When the primary DC in a traveling-wave resonator, TWR, is replaced by an NRDC, there are some interesting and useful consequences. For brevity we omit the detail analysis. In the simple case of a loop without reflections, the steady-state power gain for the forward waves (those traveling, say, counterclockwise in the loop of Fig. 1) is given by

$$M_f^2 = C_1^2/(1 - A\sqrt{1 - C_1^2}\cos\theta + A^2(1 - C_1^2))$$

where θ is the electrical length of the loop and A^2 is the relative power attenuation for a wave traversing the loop. A similar expression holds for the power gain for the backward waves in the loop, with C_2 replacing C_1. Thus, it is suggestive that the NRDC in a TWR can perform several important functions.

1) Adjusting C_1 controls the desired gain (of the forward waves).
2) Setting $C_2 = 0$, while C_1 has the value determined in (2), isolates the source from unwanted amplified internal reflections in the loop which without isolation are often the cause of great difficulty in tuning a ring.
3) Setting $C_2 = 0$, also isolates the loop from reflections from the dummy load which might be amplified in the loop.

A lengthy analysis, given elsewhere [8], of a TWR loop possessing a general source of internal reflections, and coupled by a NRDC to a source of power, verified this supposition. However, there are also some drawbacks. Unfortunately, the reflections from the dummy load would be channeled back toward the source. However, since the VSWR of these loads can be made as low as 1.1 or better, this would generally not harm the source or affect the tuning of the loop.

Another possible source of difficulty is that the internal reflection coefficient R_i is always greater for the case of $C_1 \neq 0$, and $C_2 = 0$, than for the case of reciprocal coupling $C_1 = C_2 = C$. On the other hand, the loaded Q for the buildup of the amplified backward waves is greater than the loaded Q for the forward waves when $C_1 \neq 0$, $C_2 = 0$. Thus, for the usual short-pulse operation of the ring the effect of the larger R_i is negated, somewhat, by the effect of the larger loaded Q on the buildup of the backward waves.

Acknowledgment

The author wishes to thank Profs. J. W. E. Griemsmann and M. Sucher for their valuable discussions and critical comments on this work.

Henry Berger
Dept. of Electrophysics
Polytechnic Inst. of Brooklyn
Farmingdale, N. Y.

References

[1] Montgomery, C. G., R. H. Dicke, and E. M. Purcell, *Principles of Microwave Circuits*, vol 8, M.I.T. Radiation Lab. Ser. New York: McGraw-Hill, ch 8, 1948.
[2] Damon, R. W., Magnetically controlled microwave directional coupler, *J. Appl. Phys.*, vol 26, Oct 1955, p 1281–1282.
[3] Berk, A. D., and E. Strumwasser, Ferrite directional couplers, *Proc. IRE*, vol 44, Oct 1956, pp 1439–1445.
[4] Stinson, D. C., Coupling through an aperture containing an anisotropic ferrite, *IRE Trans. on Microwave Theory and Techniques*, vol MTT-5, Jul 1957, pp 184–191.
[5] Fox, R. H., A nonreciprocal four-pole ring circuit, Tech Rept 68, M.I.T. Lincoln Lab., Lexington, Mass., Sep 1954.
[6] Davison, B., Multi-element ferrite device, *1957 IRE WESCON Conv. Rec.*, vol. 1, pt 1, pp 39–51.
[7] Skeie, H., Nonreciprocal coupling with single-crystal ferrites, *IEEE Trans. on Microwave Theory and Techniques*, vol MTT-12, Nov 1964, pp 587–594.
[8] Berger, H., The general theory of nonreciprocal directional couplers and applications in TWR circuits, Research Rept PIBMRI-1110-63, Polytechnic Inst. of Brooklyn, N. Y., Mar 1963.

An Optical All-Pass Network

Introduction

The problem of maintaining the correct relative phase shift between the modulation envelope components of a modulated coherent optical signal will, in all probability, eventually assume the same importance at optical frequencies that it does today at radio and microwave frequencies. Well-known phase-correcting techniques at radio frequencies are based on the application of all-pass lumped-parameter networks [1], generally constructed of inductors and capacitors in lattice and bridged-T configurations. Strip-line and transmission-line equivalents have been proposed for microwave applications [2]. Direct realization of optical all-pass filters by means of these techniques appears to be formidable. Reference [3] discusses a number of relatively unexploited microwave techniques, including the resonator-circulator principle [4] utilized in this optical all-pass device.

Manuscript received December 14, 1964. The research reported here was supported by the U. S. Air Force under Contract AF33(615)-1593.

Optical Circulator

The circulator, illustrated schematically in Fig. 1, is similar to that proposed by S. Saito, et al. [5]. It consists of a polarizing prism beam splitter [6], a magneto-optic medium and a loss-free reflector.

The Resonator and the Reflected Wave

Consider a Fabry-Perot-like cavity of length d formed with a highly reflecting mirror on one side and a low-loss multilayer dielectric transmitting-reflecting film laid on a transparent plate on the other (Fig. 2). If a plane optical wave of unit amplitude impinges normal to the left face of the plate, then the total reflected wave, as measured at the left-hand surface of the plate is given by

$$E_R = \frac{S_{11} + (S_{11}S_{22} - S_{12}^2)e^{-i\theta}}{1 + S_{22}e^{-i\theta}}. \quad (1)$$

In (1), S_{11} and S_{22} are the (complex) reflection coefficients as seen from the left and right sides of the plate-film structure, respectively, S_{12} is the (complex) transmission coefficient, and

$$\theta = 2\frac{\omega d}{c}, \quad (2)$$

where c is the velocity of light in the intervening medium and d is the thickness of the medium (see Fig. 2). If the dielectric film is loss free, then the matrix of the scattering coefficients has the property [7]

$$[S]\,[S]^* = [I] \quad (3)$$

where [I] is the unit matrix. It follows from (3) that[1]

$$E_R = -\left(\frac{S_{12}}{S_{12}^*}\right)e^{-i\theta}\left[\frac{1 + S_{22}^* e^{i\theta}}{1 + S_{22}e^{-i\theta}}\right] \quad (4)$$

or

$$E_R = \exp i\left\{(\theta + \psi_{12}) + 2\tan^{-1}\left[\frac{R\sin(\theta + \psi_{22})}{1 + R\cos(\theta + \psi_{22})}\right]\right\} \quad (5)$$

where ψ_{12} is the phase of S_{12}, ψ_{22} is the phase of S_{22}, and R is the magnitude of S_{22}. Since $|E_R| = 1$ and $\arg(E_R)$ is a function of frequency, E_R has the properties of a phase dispersive all-pass filter.

Equation (6) can be put in a more tractable form by writing ω as a departure $\Delta\omega$ from center frequency ω_0,

$$\omega = \omega_0 + \Delta\omega. \quad (6)$$

[1] It is assumed that phase is reversed at the right-hand reflector and that the phase of the scattering coefficients vary relatively slowly with frequency.

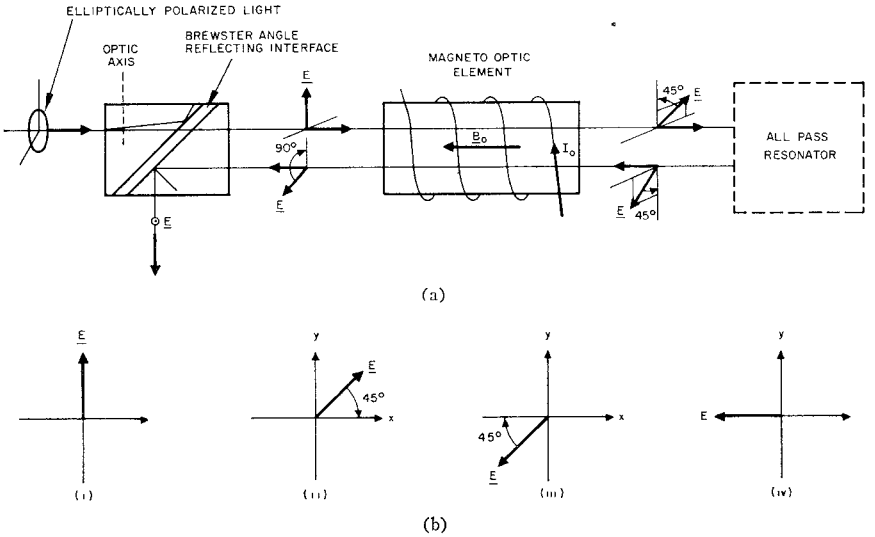

Fig. 1. Optical circulator. (a) Schematic diagram. (b) Position of electric vector (i) before entering magneto-optic element (ii) after leaving magneto-optic element (iii) after reflection (iv) after second pass through magneto-optic element.

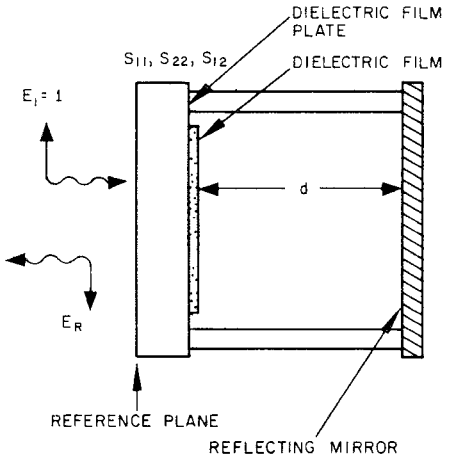

Fig. 2. The resonant cavity.

If d/c satisfies a resonance condition at ω_0, viz.,

$$2\omega_0(d/c) = (2n+1)\pi - \psi_{22}, \quad n \text{ an integer} \tag{7}$$

then we find

$$E_R = \exp\left\{-i\left[\delta + 2\tan^{-1}\left(\frac{R\sin\delta}{1-R\cos\delta}\right)\right]\right\} \tag{8}$$

where

$$\delta = \frac{2\Delta\omega}{c}d = \frac{\Delta\omega}{\omega_0}[(2n+1)\pi - \psi_{22}]. \tag{9}$$

If the phase of E_R is denoted by $\beta(\omega)$, then the associated group delay is

$$T(\Delta\omega) = \frac{d\beta}{d(\Delta\omega)} = \frac{2R\dfrac{d}{c}}{(1-R)^2}\left[\frac{(\cos\delta - R)}{1+\dfrac{4R}{(1-R)^2}\sin^2\dfrac{\delta}{2}}\right]. \tag{10}$$

The Small Deviation (or Lumped-Parameter) Approximation

Fully evolved synthesis procedures exist for lumped-parameter all-pass networks and, therefore, it is advantageous to cast our expression (10) into the lumped-parameter all-pass form.

The important region of the group delay curve lies in the range $0 \leq \delta \leq \cos^{-1} R$. If R is close to 1, then over this range $\delta \ll 1$. Thus, to an approximation

$$T(\Delta\omega) \approx \frac{2\dfrac{d}{c}R}{(1-R)^2}\left[\frac{(1-R)-\dfrac{\delta^2}{2}}{1+\dfrac{R}{(1-R)^2}\delta^2}\right], \tag{11}$$

which reduces to the standard form of the group delay function of the lumped-parameter all-pass network,

$$T(\Delta\omega) \approx \frac{2/\sigma_0}{1+(\Delta\omega/\sigma_0)^2}, \tag{12}$$

if

$$\delta/\sqrt{2(1-R)} \ll 1.$$

Consider a case wherein $R = 99$ per cent. Figure 3 illustrates that the differences between the delay functions of the associated optical and equivalent lumped-parameter normalized delay functions [(10) and (12)] over the range

$$0 < \frac{(\Delta\omega)2d}{c} < 10^{-1} \tag{13}$$

are quite small.

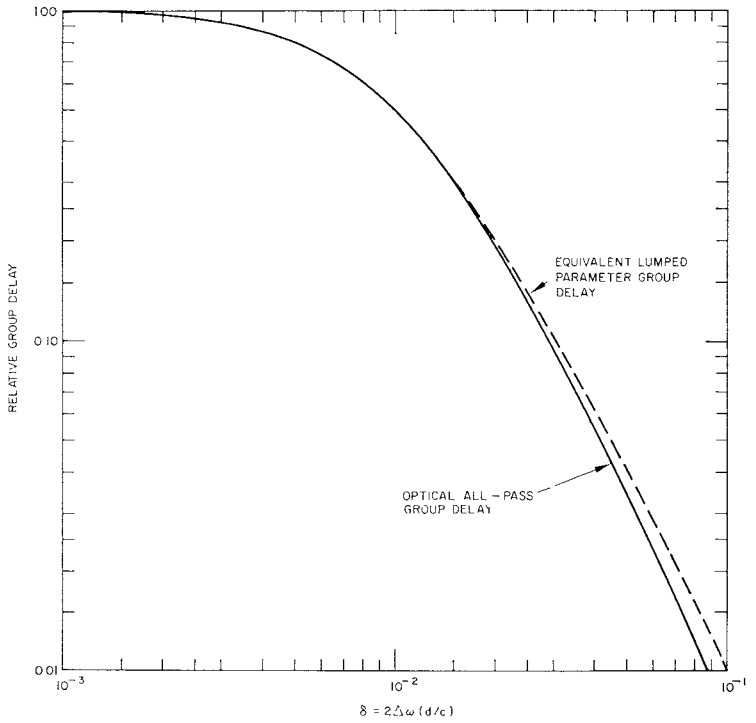

Fig. 3. The optical all-pass group delay function for a cavity reflector reflectivity of 99 per cent.

Required Precision in Adjustment

If we differentiate (9), we find that small changes in length Δd are related to small changes in center frequency $\Delta\omega_0$, by the equation

$$\Delta d \approx -\frac{c}{\omega_0^2}\left(\frac{2n+1}{2}\right)\pi\Delta\omega = -\frac{d_0}{\omega_0}\Delta\omega \quad (14)$$

where d_0 is the nominal cavity length. Thus, for example, with $R=99$ per cent, Fig. 3 indicates that a displacement $\Delta\delta = 5\times 1.0^{-3}$ rad is sufficient to cause about a 20 per cent delay variation in the delay characteristic. To maintain even this control requires an adjustment and temperature stability capability that corresponds to a cavity variation

$$\Delta d \approx 0.0025\lambda_0! \quad (15)$$

A. D. Jacobson
T. R. O'Meara
Hughes Research Lab.
Malibu, Calif.

References

[1] Storer, J. E., *Passive Network Synthesis*. New York: McGraw-Hill, pp 130–137.
[2] Steenaart, W. J. D., The synthesis of coupled transmission line all-pass networks in cascades of 1 to *n*, *IEEE Trans. on Microwave Theory and Techniques*, vol MTT-11, Jan 1963, pp 23–29.
[3] Cohn, S. B., and E. N. Torgow, Investigation of phase and time delay equalizers, Rept 1, Rantec Project No. 40223, Rantec Corp., Calabasas, Calif., Aug 1964.
[4] O'Meara, T. R. and A. D. Jacobson, The resonator circulator all-pass network, Part I: Microwave realizations, Part II: Optical realizations, Hughes Research Rept. 334, Apr 1965.
[5] Saito, S., K. Yokoyama, and Y. Fujii, A light circulator using the Faraday effect of heavy flint glass, *Proc. IEEE (Correspondence)*, vol 52, Aug 1964, p 979.
[6] Archard, J. F., and A. M. Taylor, An improved Glan-Foucault prism, *J. Sci. Instr.*, vol 25, Dec 1948, p. 407–409.
[7] Mathews, E. W., Jr., The use of scattering matrices in microwave circuits, *IRE Trans. on Microwave Theory and Techniques*, vol MTT-3, Apr 1955, pp 21–26.

A Variable Characteristic Impedance Coaxial Line

Abstract

The development of Time Domain Reflectometry (TDR) for UHF and microwave impedance measurements in coaxial systems has created a problem of calibrating the TDR system for accurate measurements of small reflections. A need for coaxial impedance standards has been resolved by the development of a variable impedance device which can be calibrated by the use of fixed coaxial standards.

This correspondence deals with the design and analysis of a variable impedance line. This line is described and its performance characteristics are discussed. Its measured characteristic impedance is compared at discrete points with the impedance obtained from empirical and approximate theoretical formulas.

Introduction

Until now, slotted lines and frequency domain reflectometers have been the two principal tools for UHF and Microwave Impedance Measurements. Recently, the development of TDR has enabled the measurements engineer to obtain information about the broadband impedance characteristics of coaxial lines and components almost at a glance. The TDR systems have been calibrated for accurate measurements of small reflections ($|\Gamma| < 0.005$) by the use of fixed coaxial impedance standards. A variable characteristic impedance device eliminates the inconvenicnce of inserting and removing fixed standards. Such a device has been constructed and analyzed.

Manuscript received April 5, 1965.

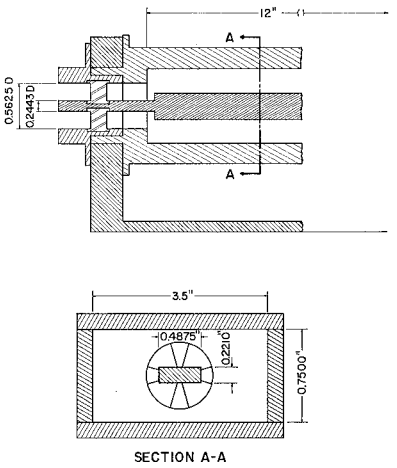

Fig. 1. Cutaway view of variable impedance rectangular line.

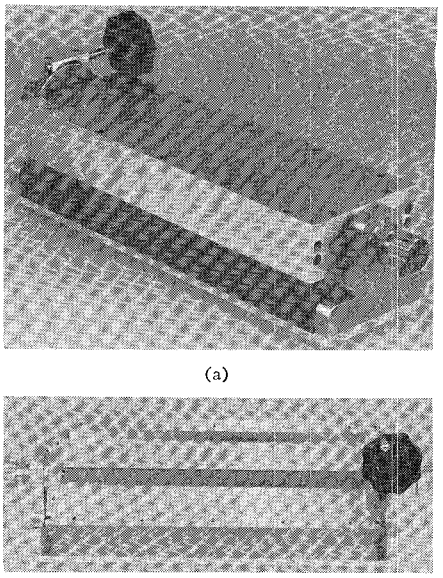

(a)

(b)

Fig. 2. (a) Photograph of variable impedance rectangular line. (b) Photograph of variable impedance rectangular line.

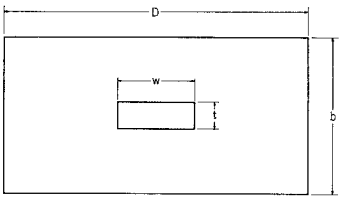

Fig. 3. Geometry of a rectangular coaxial line.

Design and Description

The variable impedance line discussed here is a rectangular coaxial transmission line with a stationary inner conductor and a rotating outer conductor. A worm gear drives the outer conductor through an angular range greater than 180°. Figure 1 is a cutaway view of the variable impedance line while Fig. 2 is a photograph of the exterior and interior of the line. When the conductors are aligned in the parallel plane configuration of Fig. 3, the notation used by other authors [1], [2], is suitable. Using the curves of Bates [1] and the configuration of Fig. 3, parameters of $w/b=0.650$ and $t/b=0.295$ with $b=0.750$ inch yield a characteristic impedance of 55 ohms. The width D is sufficiently great that it may be considered infinite and, hence, does not enter into the calculation of Z; this line was constructed. On rotating the outer conductor through 90° and reversing the parameters, the same curves indicate an impedance of 44 ohms. This was the required range for the variable impedance line.

Performance Characteristics

The characteristic impedance of the variable impedance line was measured as a function of angle of rotation by means of a TDR system. Calibration of the system was accomplished by means of circular coaxial standards whose characteristic impedances were determined from

$$Z_s = \frac{59.958}{\sqrt{\epsilon}} \ln\left(\frac{d}{a}\right), \quad (1)$$

where, of course, d is the inner diameter of the outer conductor, a is the outer diameter of the inner conductor, ϵ is the relative dielectric constant of the medium, and Z_s is the characteristic impedance of the circular coaxial line.

Once the characteristic impedance Z_s of the fixed standard is known, the reflection coefficient Γ_s can be calculated from the usual relationship

$$\Gamma_s = (Z_s - Z_0)/(Z_s + Z_0). \quad (2)$$

Here Z_0 is a theoretical characteristic impedance which for the purpose of this experiment was 50 ohms. All subsequent reflection coefficients were also determined with respect to the same 50-ohm level.

If the reflection coefficient Γ_s is known, Γ_u the unknown reflection coefficient of the